



Cite this: *Nanoscale*, 2016, **8**, 8955

## Coiled coil interactions for the targeting of liposomes for nucleic acid delivery†

Erik E. Oude Blenke,<sup>a</sup> Joep van den Dikkenberg,<sup>a</sup> Bartjan van Kolck,<sup>b</sup> Alexander Kros<sup>b</sup> and Enrico Mastrobattista<sup>\*a</sup>

Coiled coil interactions are strong protein–protein interactions that are involved in many biological processes, including intracellular trafficking and membrane fusion. A synthetic heterodimeric coiled-coil forming peptide pair, known as E3 (EIAALEK)<sub>3</sub> and K3 (KIAALKE)<sub>3</sub> was used to functionalize liposomes encapsulating a splice correcting oligonucleotide or siRNA. These peptide-functionalized vesicles are highly stable in solution but start to cluster when vesicles modified with complementary peptides are mixed together, demonstrating that the peptides quickly coil and crosslink the vesicles. When one of the peptides was anchored to the cell membrane using a hydrophobic cholesterol anchor, vesicles functionalized with the complementary peptide could be docked to these cells, whereas non-functionalized cells did not show any vesicle tethering. Although the anchored peptides do not have a downstream signaling pathway, microscopy pictures revealed that after four hours, the majority of the docked vesicles were internalized by endocytosis. Finally, for the first time, it was shown that the coiled coil assembly at the interface between the vesicles and the cell membrane induces active uptake and leads to cytosolic delivery of the nucleic acid cargo. Both the siRNA and the splice correcting oligonucleotide were functionally delivered, resulting respectively in the silencing or recovery of luciferase expression in the appropriate cell lines. These results demonstrate that the docking to the cell by coiled coil interaction can induce active uptake and achieve the successful intracellular delivery of otherwise membrane impermeable nucleic acids in a highly specific manner.

Received 26th January 2016,

Accepted 20th March 2016

DOI: 10.1039/c6nr00711b

www.rsc.org/nanoscale

## Introduction

Coiled coil domains are structural motifs found in proteins of 2–7  $\alpha$ -helical strands that are coiled around each other.<sup>1–4</sup> The primary structure is typically composed of multiple heptad repeat amino acid sequences (denoted as *abcdefg*) in which the *a* and *d* residues are non-polar and create the hydrophobic core of the coil. The *e* and *g* positions are charged residues that introduce electrostatic interaction and specificity between

opposing coils.<sup>5</sup> Coiled coil interactions are involved in many biological processes, including intracellular trafficking and membrane fusion, mainly mediated by SNARE proteins (soluble *N*-ethylmaleimide-sensitive factor attachment protein receptor).<sup>6,7</sup>

In nanomaterial research, synthetic coiled coil motifs have been used to create a tunable system for the controlled display of ligands on nanoparticles,<sup>8–10</sup> defined architectures,<sup>11,12</sup> and for the self-assembly of polymer–peptide hybrid systems.<sup>13–17</sup> The group of Kopeček used coiled coil peptides on a HPMa polymer scaffold as a means to induce highly specific antigen crosslinking on malignant B cells both *in vitro* and *in vivo*.<sup>18–21</sup> These examples demonstrate the versatile application of coiled-coils as surface modifications for molecular recognition and their potential as signaling molecules on complex surfaces such as the cell membrane.

In this study, the aim is to investigate the potential of synthetic coiled coil peptides for liposomal drug delivery purposes. To this end, two synthetic, parallel coiled coil forming peptide sequences are used that are referred to as K3 (KIAALKE)<sub>3</sub> and E3 (EIAALEK)<sub>3</sub> (three repeats of lysine-rich and glutamic acid-rich heptads). Originally they have been designed as affinity tags for recombinant protein purifi-

<sup>a</sup>Department of Pharmaceutics, Utrecht Institute of Pharmaceutical Sciences (UIPS), Utrecht University, Universiteitsweg 99, 3584 CG Utrecht, The Netherlands.

E-mail: e.mastrobattista@uu.nl; Fax: +31 302517839; Tel: +31 622736567

<sup>b</sup>Supramolecular and Biomaterials Chemistry, Leiden Institute of Chemistry, Leiden University, Einsteinweg 55, 2333 CC Leiden, The Netherlands

† Electronic supplementary information (ESI) available: Two videos of the experiment are shown in Fig. 5, demonstrating the distinctive characteristics of the peptide pair in a mixed population of cells are available in online. Video S1 shows the experiment in the bright field channel including the green channel (calcein-AM stained unfunctionalized cells) and orange channel (rhodamine labeled liposomes). Video S2 shows the exact same frames but combining the fluorescent channels only, including the blue channel for Hoechst nuclear staining. Both videos consist of 31 frames at a frame rate of 5 fps. The labeled liposomes are injected after frame 1. The videos span a total timeframe of 15 minutes. See DOI: 10.1039/c6nr00711b

cation.<sup>22,23</sup> Inspired by their natural role in membrane fusion, coiled coil sequences have been previously used to mimic a system where liposomal membranes fuse upon coiling of the two complementary peptides.<sup>24–26</sup> Recent work showed that the peptide could be incorporated into a cellular membrane by conjugating it to a hydrophobic moiety. Subsequently, liposomes that were functionalized with the opposing coil could be targeted to these cells, as was demonstrated for several cell lines and zebra-fish embryos.<sup>27–29</sup> In the present work we use the K3/E3 combination to specifically dock stable nucleic acid lipid particles to the target cell and achieve intracellular delivery. Nucleic acid drugs, like siRNA or splice correcting antisense oligonucleotides (SCO) have the potential to modulate disease pathways on the transcriptional level, but due to their large size and negatively charged backbone they cannot reach their intracellular site of action. Therefore they require a delivery vehicle such as the liposomes used here. Liposomes are lipid vesicles that protect the oligonucleotides from degradation and can help to deliver them to their intracellular target site, but they do require further surface modification to get access to the target cell. In the work presented here, the lipid vesicles were functionalized with either K3 or E3 coil peptides and the cell surface was modified by insertion of the complementary peptide using a hydrophobic anchor. The assembly of the K3/E3 coiled coils at the cell surface was shown to initiate endocytosis and to eventually achieve the functional delivery of two types of membrane impenetrable oligonucleotides. This poses a novel alternative to viral carriers or lipid/polymer based transfection reagents that are either associated with toxicity/immunogenicity, or are highly unspecific. Live cell confocal imaging was used to monitor peptide-specific docking over time and revealed that this happens in a very short timeframe and with a very high distinctive character, demonstrating the high affinity and specificity of the used peptide pair.

## Experimental section

### Materials

Diioleoylphosphatidylethanolamine (DOPE), 1,2-dioleoyl-3-dimethylammonium-propane (DODAP), *N*-palmitoyl-sphingosine-1-succinyl[methoxy(polyethylene glycol)2000] (C16 Ceramide-PEG2000), 1,2-distearoyl-*sn*-glycero-3-phosphoethanolamine-*N*-[maleimide(polyethylene glycol)-2000] (DSPE-PEG2000-maleimide), and 1- $\alpha$ -phosphatidylethanolamine-*N*-(Lissamine Rhodamine B sulfonyl) (Rho-PE) were from Avanti Polar Lipids (Alabaster, AL, USA). Cholesterol was from Sigma-Aldrich (St. Louis, MO, USA).

The siRNA sequences directed against luciferase are as follows: sense 5'-CUUACGCUGAGUACUUCGAdTdT-3'; antisense 5'-UCGAAGUACUCAGCGUAAGdTdT-3'. Antisense oligonucleotide Luc705 is made of all phosphorothioate bases 5'-CCUCUUACCUCAGUUACA-3' (underlined bases are 2'-O-methyl modified). All oligonucleotides were provided by Glaxo-SmithKline (Stevenage, UK) for use within the EU IMI

COMPACT consortium. Cysteine modified K3 and E3 peptides (Ac-CKIAALKEKIAALKEKIAALKE-NH<sub>2</sub> and Ac-CEIAALEKEIAALEKEIAALEK-NH<sub>2</sub>) were ordered in >90% purity from GenScript Corp. (Piscataway, NJ, USA). Lipidated peptides cholesterol-PEG<sub>12</sub>-K3 and cholesterol-PEG<sub>12</sub>-E3 (CPK and CPE) were synthesized as described before.<sup>25</sup>

### Liposome preparation

Stable nucleic acid–lipid particles are prepared using the preformed vesicle method of Maurer *et al.*<sup>30</sup> using a lipid composition of DODAP/DOPE/cholesterol/C16 Ceramide-PEG2000 at a ratio of 26/22/46/6.

For labeled vesicles, 0.5% Lissamine Rhodamine-PE was included. Using a rotary evaporator, a dry lipid film of 40  $\mu$ mol total lipid was created in a round bottom flask. After flushing with nitrogen, the lipid film was hydrated in 70% citrate buffer 50 mM pH 4.0 and 30% ethanol to a lipid concentration of 8 mM. The hydrated lipids were extruded through 100 nm pore-sized filters (Nuclepore, Pleasanton, CA, USA) using a Lipex™ Extruder (Northern Lipids, Burnaby, BC, Canada) for 10–12 times. Nucleic acids (NA) (splice correcting oligo or siRNA) were dissolved in 70% citrate buffer 50 mM pH 4.0 and 30% ethanol. Both the vesicles and the NA solution were preheated to 37 °C and then mixed together under continuous heavy stirring in a final NA/lipid ratio of 0.06 (wt/wt). The mixture was then incubated for 1 hour at 37 °C to allow reorganization of the vesicles. Ethanol was removed and the buffer was replaced by overnight dialysis in a 10 K MWCO Slide-A-Lyzer G2 Dialysis Cassette (Life Technologies) at 4 °C against PBS. Unloaded vesicles were dialyzed directly after extrusion. After dialysis, loaded vesicles were subjected to three rounds of ultracentrifugation in a Type 70.1 Ti rotor for 50 minutes at 55 000 rpm at 4 °C to wash away unencapsulated NA.

### Insertion of K3- and E3-peptides into the formulated vesicles

To reduce the C-terminal cysteine thiol groups, K3 and E3 peptides were incubated with Immobilized TCEP Disulfide Reducing Gel (Pierce #77712) for 1 hour at room temperature and then separated from TCEP gel slurry by centrifugation in paper filter spin cups (Pierce #69700). Immediately afterwards they are added to DSPE-PEG2000-maleimide micelles, dispersed in PBS pH 7.4, in a 1 : 1 molar ratio of thiol : maleimide and incubated overnight at 4 °C. For insertion of the peptide micelles into the vesicles,<sup>31</sup> the vesicles and the micelles are preheated to 45 °C. The K3 or E3 micelles were then added to the vesicles in a 1 : 100 molar ratio and incubated overnight at 45 °C (extrapolated from the total amount of phospholipids, measured as described below). To remove the uninserted micelles, the resulting vesicles were subjected to three rounds of ultracentrifugation in a Type 70.1 Ti rotor for 50 minutes at 55 000 rpm at 4 °C.

### Characterization of vesicles

To separate the lipids from the NA, samples are extracted according to Bligh and Dyer.<sup>32</sup> The top phase of the extraction was collected and evaporated using a centrifugal concentrator.

When completely dry, the samples were reconstituted in MilliQ water and the amount of nucleic acid was measured by UV/VIS spectrophotometry at 260 nm using a NanoDrop 1000 spectrophotometer (Thermo Scientific). The lipid fraction in chloroform was assayed for the total phosphate amount according to the method of Rouser using sodium biphosphate as a standard.<sup>33</sup> The total lipid amount was then extrapolated from the amount of phospholipid (DOPE) present in the formulation. The encapsulation efficiency was calculated using the formula

$$\text{Encapsulation efficiency(\%)} = \frac{\frac{[\text{oligonucleotides}]_{\text{after ultracentrifugation}}}{[\text{phospholipids}]_{\text{after ultracentrifugation}}}}{\frac{[\text{oligonucleotides}]_{\text{before dialysis}}}{[\text{phospholipids}]_{\text{before dialysis}}}} \times 100$$

The hydrodynamic diameter and the polydispersity index were measured by dynamic light scattering, using a Malvern CGS-3 multiangle goniometer with a He-Ne laser source ( $\lambda = 632.8$  nm, 22 mW output power) under an angle of  $90^\circ$  (Malvern Instruments, Malvern, UK). The zeta-potential of the liposomes was measured using laser Doppler electrophoresis on a Zetasizer Nano-Z (Malvern Instruments) with samples dispersed in 10 mM Hepes buffer pH 7.4 (no additional salts).

#### Aggregation assay

To demonstrate that the peptides are freely accessible on the distal end of the inserted PEG-lipids, the peptide mediated aggregation of the vesicles is measured by dynamic light scattering as described above. The vesicles were diluted to 25 nM phospholipid in PBS and the hydrodynamic diameter was measured every minute for a total of 25 minutes. K3- and E3-functionalized vesicles were mixed together and immediately afterwards the measurement was started. K3- and E3-functionalized vesicles were mixed with unfunctionalized vesicles as controls.

#### Cell culture

For antisense oligo delivery, HeLa cells expressing the luciferase gene interrupted by mutated human  $\beta$ -globin intron 2 (IVS2-705) (HeLa pLuc705) were used.<sup>34</sup> For siRNA delivery HeLa cells stably transfected with a EGFPLuciferase gene under the PGK-promoter were used (construct described here<sup>35</sup>). All cells were cultured in Dulbecco's Modified Eagle's Medium with high glucose supplemented with 10% (v/v) fetal bovine serum and penicillin-streptomycin-amphotericin B at  $37^\circ\text{C}$  under a humidified atmosphere containing 5%  $\text{CO}_2$ . The medium for the HeLa pLuc705 cell line also contained  $200 \mu\text{g ml}^{-1}$  of hygromycin B. All media and supplements were from Sigma-Aldrich. Cells were regularly tested for mycoplasma and all cell lines used were found to be negative.

#### Microscopy

10 000 HeLa pLuc705 cells were seeded per channel of an Ibidi  $\mu$ -Slide VI<sup>0.4</sup> (Ibidi GmbH, Munich, Germany) one day prior to

the addition of the vesicles. On the day of the experiment, cells were washed with PBS once and incubated with  $5 \mu\text{M}$  CPE or CPK in OptiMEM medium without phenol red (Life Technologies) for 5 minutes at  $37^\circ\text{C}$ . As a control OptiMEM medium without the peptides was used. Cells were washed with PBS and incubated with rhodamine labeled vesicles ( $125 \mu\text{M}$  phospholipid) in OptiMEM for 10 minutes at  $37^\circ\text{C}$ . Cells were washed with PBS and incubated in OptiMEM containing  $1 \mu\text{g ml}^{-1}$  Hoechst 33342 (Life Technologies, Bleiswijk, Netherlands) and incubated for 15 minutes at  $37^\circ\text{C}$ . Cells were washed with PBS and immediately imaged in OptiMEM on a Keyence BZ-9000 fluorescence microscope (Keyence, Düsseldorf, Germany) using a Nikon CFI Plan APO VC  $60\times$  oil immersion lens (NA 1.4 WD 0.13). Overlay pictures were made in BZ-II Analyzer software (Keyence). For uptake studies, cells were incubated on separate slides at  $37^\circ\text{C}$  for an additional 1 or 4 hours and then washed and imaged. No nuclear staining was applied in these studies.

To test the distinctive character of the peptide pair, 10 000 HeLa pLuc705 cells were seeded in a  $\mu$ View clear-bottom 96 well plate (Greiner Bio-One B.V. Alphen aan de Rijn, Netherlands). Next day, nuclei were stained as described above and after aspiration of the medium, the middle of the well was blocked with a piece of Teflon (PTFE) tube, with an outer diameter of 3 mm. The area outside the tube was incubated with CPE as above and after washing, the ring barrier was removed and the whole well was incubated with rhodamine labeled K-functionalized vesicles ( $125 \mu\text{M}$  phospholipid). After washing, the cells were incubated in OptiMEM and imaged in a Yokogawa Cell Voyager 7000 (Yokogawa, Tokyo, Japan) (see the inset in Fig. 4 for a schematic view).

A similar experiment was performed with cells in suspension. For this cells were stained with Hoechst as described above and then split in separate vials. These were incubated separately with CPE or OptiMEM with 250 nM of calcein-AM (Life Technologies) for 5 minutes at  $37^\circ\text{C}$ . In between incubation steps cells were washed with PBS using centrifugation at 250g for 3 minutes. After this the two vials were combined and 10 000 cells were then transferred to a  $\mu$ View clear-bottom 96 well plate and imaged while still in suspension in the Cell Voyager. An equal volume of K3-functionalized rhodamine-labeled vesicles (final concentration of  $125 \mu\text{M}$  total lipid) was injected 30 seconds after the onset of the live cell imaging using a built-in dispenser. A picture was taken every 30 seconds over a time period of 15 minutes. These pictures were converted into a time-lapse movie with 5 frames per second. See ESI Videos 1 and 2.†

#### Transfection studies

Transfection studies were done in 24 well plates, with HeLa pLuc705 cells seeded at a density of 45 000 cells per well and HeLa PGK-EGFPLuciferase cells at a density of 35 000 cells per well 24 h before transfections. On the day of the experiment, cells were washed once with PBS and half of the wells were incubated with  $5 \mu\text{M}$  CPE or CPK in OptiMEM and the other half with plain OptiMEM for 5 minutes at  $37^\circ\text{C}$ . Cells were

washed with PBS and incubated with SCO or siRNA loaded vesicles (1  $\mu$ M oligonucleotides) in OptiMEM for 4 hours at 37 °C. Afterwards, transfection mixtures were replaced by the complete medium and plates were incubated for 24 hours at 37 °C. As a positive control for nucleic acid delivery, Lipofectamine 2000 (Life Technologies) was used according to the manufacturer's protocol. Each condition was measured in triplo. The following day, cells were washed once with PBS and lysed with 250  $\mu$ l of lysis buffer (Tris 25 mM, EDTA 2 mM, 1% Triton X-100, 10% glycerol) on a shaking board at 37 °C for 10 minutes. For each well, 50  $\mu$ l of lysate was mixed with 50  $\mu$ l of Luciferase Assay Reagent (Promega, Leiden, Netherlands) in triplo. The reagent was injected using a FLUOstar OPTIMA microplate reader (BMG Labtech, Ortenberg, Germany) equipped with an injection pump. 2 seconds after injection, luminescence was measured for 10 seconds according to the supplier's recommendation. Results are plotted as mean plus standard deviation in GraphPad Prism 6. Statistical analysis was performed using multiple paired *t*-tests. Statistical significance is denoted as \*\*\* with *p* < 0.001.

## Results

### Formulation of stable nucleic acid vesicles with high loading

The stable nucleic acid lipid particles used here were prepared by the preformed vesicle method.<sup>30</sup> In this procedure, ethanol is used to destabilize the preformed empty unilamellar vesicles which enables entrapment of the nucleic acids. The vesicles used here consist of DOPE/DODAP/cholesterol/C16 Ceramide-PEG2000 at a molar ratio of 22/26/46/6. DODAP is a lipid with a positive charge at pH of formulation which is necessary for interaction with the nucleic acids and with the predominantly negatively charged cell membrane.<sup>30,36</sup> DOPE is a so called 'helper lipid', that prefers to adopt the inverted hexagonal ( $H_{II}$ ) phase which favors intracellular delivery.<sup>36</sup> A PEG-lipid with the Ceramide C16 anchor was used, because it is known to dissociate from the bilayer.<sup>37</sup> The diameter of unfunctionalized vesicles is ~80 nm and their zeta potential is almost neutral due to the PEG-lipids (Table 1).

Two types of nucleic acids were encapsulated in two separate batches of liposomes, a double stranded siRNA against luciferase and a single stranded splice correcting oligonucleotide (SCO) that corrects the splicing of luciferase pre-mRNA in the HeLa pLuc705 cell line.<sup>34</sup> The nucleic acids that were not encapsulated were removed from the vesicles by ultracentrifugation and the encapsulation efficiency was calculated,

**Table 1** Basic characteristics of the unloaded vesicles (averages and standard deviation of three measurements)

Sample	Size	PDI	Zeta potential
Unfunctionalized vesicles	83.6 $\pm$ 0.6	0.06	-3.4 $\pm$ 0.3
E3-functionalized vesicles	97.4 $\pm$ 1.3	0.08	-7.7 $\pm$ 0.6
K3-functionalized vesicles	96.6 $\pm$ 0.7	0.07	-7.2 $\pm$ 0.7

**Table 2** Encapsulation efficiencies for the different types of nucleic acids (averages and standard deviation of three different formulations)

Nucleic acid	Encapsulation efficiency
siRNA	92.4% $\pm$ 4.2%
SCO	87.1% $\pm$ 5.4%

and corrected for the total amount of phospholipids. The encapsulation efficiencies for both types of nucleic acids are generally high, with values around 90% encapsulation on average which is typical for this preparation method<sup>30</sup> (Table 2).

### Insertion of the coiled coil forming peptides into the lipid vesicles

The formulated liposomes were functionalized with the coiled coil forming peptides K3 C(KIAALKE)<sub>3</sub> and E3 C(EIAALEK)<sub>3</sub>. The peptides are covalently coupled to a DSPE-PEG2000-maleimide lipid *via* a thioether bond, on the N-terminal cysteine (see Fig. 1). The formed peptide micelles are then inserted into the vesicles using the 'post-insertion method'.<sup>31</sup> These vesicles are functionalized with 1% of the total lipids in the outer layer by being coupled to a peptide. The insertion of the peptides is reflected by an increase in hydrodynamic diameter to ~100 nm and a small change in the zeta potential (Table 1).

### Rapid clustering and aggregation of complementary functionalized vesicles

To demonstrate that the conjugated peptides are functional and accessible, the size increase and aggregation were monitored when the two populations of vesicles were mixed together. The two individual populations were stable when stored, but when mixed together, they quickly agglomerated into bigger clusters. An increase in turbidity was observed by the eye. Dynamic light scattering measurements over time showed a gradual increase in the particle size (Fig. 2A). Immediately after mixing, particle size increased, which is in line with the high association constant of the coiled coil pair. The increase in size appeared to be bigger over time, which is explained by the exponential effect of larger particles clustering together. No size increase was seen when either of the populations were mixed together with unfunctionalized vesicles, excluding the possibility that clustering is caused by one of the peptides inserting into the membrane of other vesicles (Fig. 2B). The degree of size increase is concentration dependent with lower concentrations showing less or no size increase at all, while higher concentrations are more problematic to measure due to obscuration of the laser (data not shown). This is in line with the previous experiments where full length SNARE-driven vesicle fusion was studied showing that docking of the complementary SNAREs (and not fusion) is the rate-limiting step.<sup>38</sup> In other words, the collision and docking of two vesicles is the bottleneck in the process, which directly correlates with vesicle concentration.<sup>26</sup> This also explains why the fusion or aggregation rate of these artificial

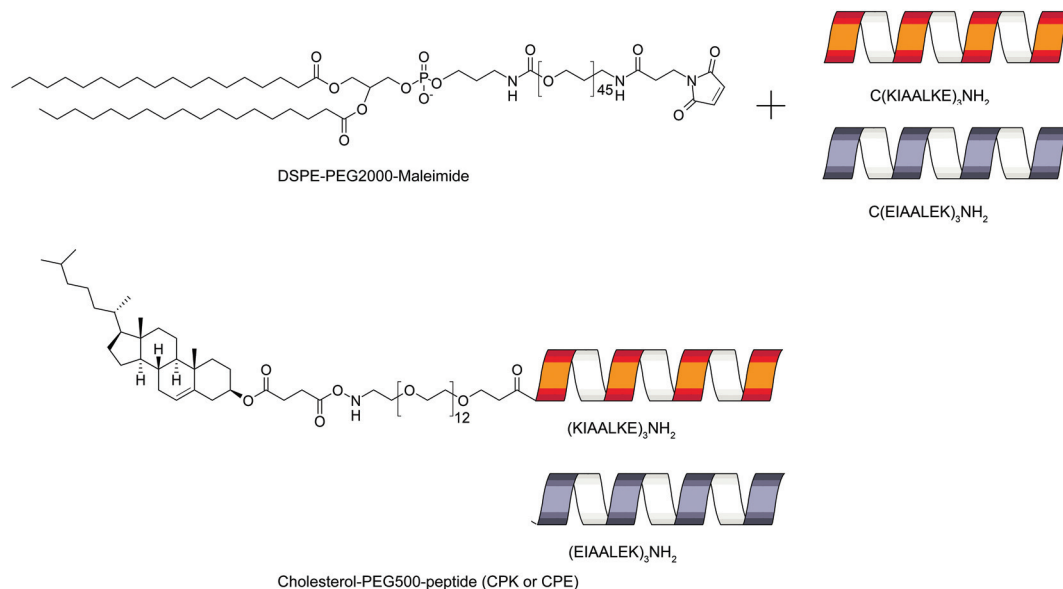


**Fig. 1** Peptide sequences and anchors used. Peptides were coupled *via* maleimide–thiol linkage to a lipid (top) or were directly conjugated to the cholesterol anchor (bottom). The lipid anchored peptides were inserted into the liposomes and the cholesterol anchored peptides were used to functionalize the cell membranes.

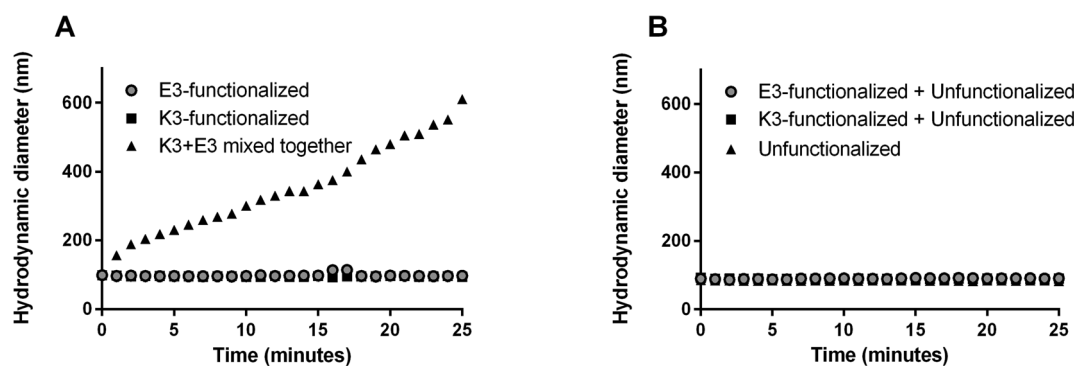


**Fig. 2** Increase in the hydrodynamic diameter of the mixed vesicles over time. Individual populations were stable in size but when the E3- and K3-functionalized vesicles were mixed together, a quick increase in size was observed.

systems is much slower (timeframes of minutes or hours, rather than (milli)seconds) than that of physiological fusion where tethering proteins facilitate the earliest vesicle contact.<sup>6,7</sup>

### Docking of the functionalized vesicles to the cell membrane

Next, it was tested whether the vesicles could also be docked to live cells using the K3/E3 coiled coil interaction. In earlier work, it was shown that using a hydrophobic anchor, both peptides could be inserted into existing membranes, either liposomal<sup>25</sup> or the membranes of living cells.<sup>27</sup> In the present work, the membranes of live HeLa pLuc705 cells were functionalized with a cholesterol anchored peptide on a short PEG spacer (cholesterol-PEG<sub>12</sub>-peptide, abbreviated as CPK and CPE, see Fig. 1). After washing, the cells were incubated with liposomes labeled with 0.5 mol% rhodamine-PE, functionalized with either the K3 or E3 peptide and then imaged using

an epifluorescence microscope. Strikingly, it was found that K3-functionalized liposomes docked to E3-functionalized cells, but not the other way around (Fig. 3).

This is in contrast with previous work that showed that both the CPE and the CPK lipopeptide could be inserted into the cellular membrane when CHO cells were used.<sup>27</sup> It should be noted that it is experimentally difficult to study whether the lipopeptide has indeed been inserted into the membrane *via* its hydrophobic anchor. However, the absence of a fluorescence signal when untreated cells are incubated with the K3-functionalized vesicles strongly indicates that the signal is dependent on the CPE peptide. Additionally, when CPE-incubated cells were incubated with E3-functionalized vesicles no fluorescence was observed, showing that the signal is dependent on heterodimeric coiled-coil formation between the K3 and E3 peptides (Fig. 3D).

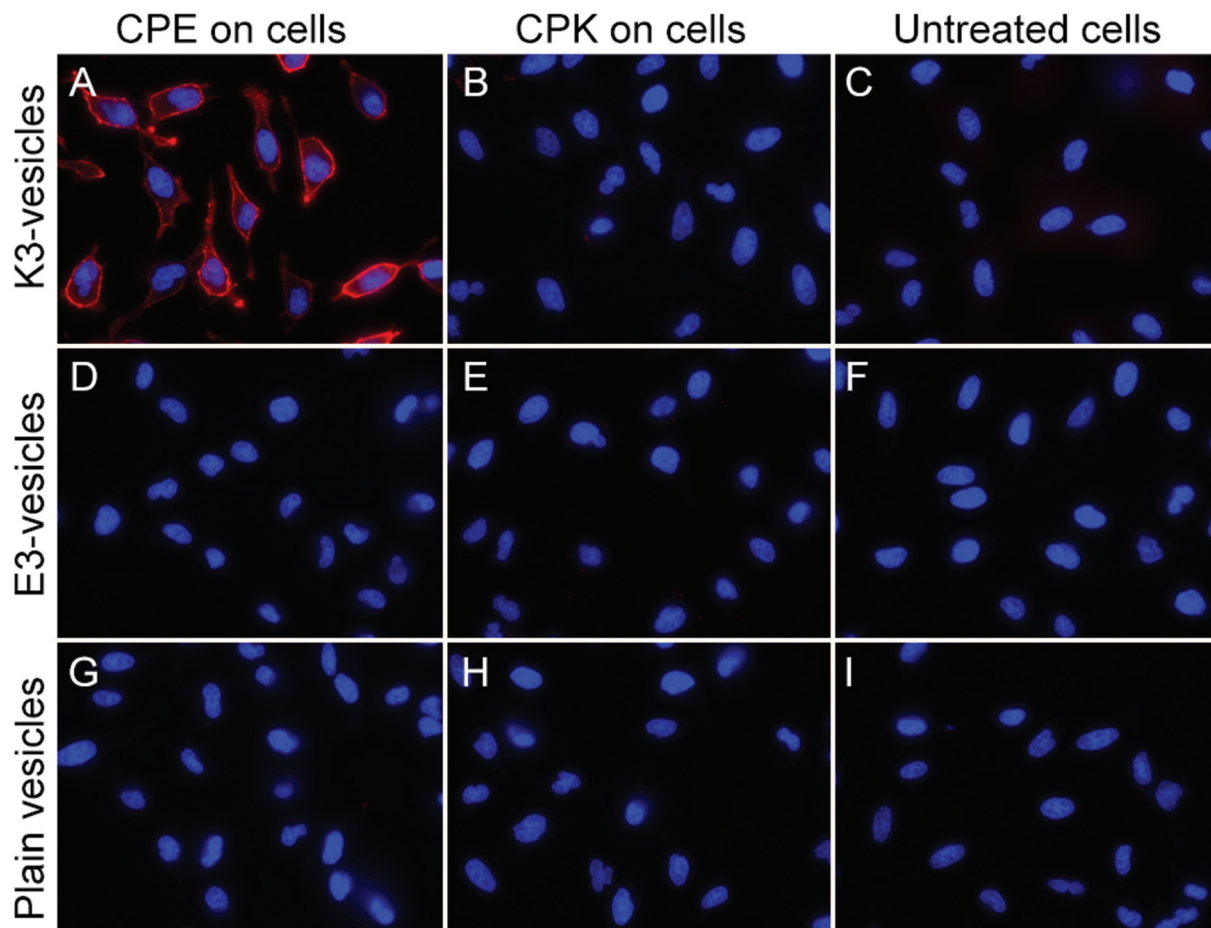


**Fig. 3** (A–I) Microscopy pictures of HeLa pLuc705 cells incubated with rhodamine-labeled vesicles. Overlay of the red and blue channels is shown for all combinations but only when CPE functionalized cells were incubated with K3-functionalized vesicles, cell binding was seen in the red channel. Nuclei were stained with Hoechst 33342 dye in the blue channel.

Similar to our results, Yano *et al.* found that when the K3 and E3 peptides were recombinantly fused to a membrane protein, only when the E3 variant was expressed, it could be fluorescently tagged by the complementary K4 peptide.<sup>39</sup> It is known that these peptides interact differently with membranes and it is likely that these interactions are also cell type dependent. The interactions of the lipidated K3 and E3 peptides with a model membrane were previously studied using surface sensitive infrared reflection absorption spectroscopy (IRRAS) and circular dichroism (CD) spectroscopy. These studies showed that peptide E3 has no interaction with the membrane whereas the K3 peptide has a much higher binding affinity for the membrane amphiphiles.<sup>40,41</sup> This is explained by the so-called snorkeling effect of K3 similar to class A peptide amphiphiles. Also, the net charge of the E3 and K3 peptides, which is  $-3$  and  $+3$  respectively, while the cellular membrane has a net negative charge, plays a role. Applying this knowledge to our findings, it is expected that the CPE lipopeptide is not hindered by charge interaction with the membrane, allowing it to insert into the membrane with its hydrophobic anchor. The CPK lipopeptide is more likely to stick to the negatively

charged glycolipids on the surface of the cell membrane, preventing insertion of the cholesterol anchor with the appropriate orientation. The peptide is then either washed away or the membrane interactions prevent it from dimerization with the complementary peptide. The microscopy images show that the interaction of the K3-functionalized vesicles with the untreated cell membrane is not strong enough to bind the liposomes to the cell membrane after the washing steps, as evidenced by the lack of a fluorescence signal (see Fig. 3B and C). Only the coiled coil interaction of the CPE and K3-functionalized vesicles is strong enough to unequivocally label the membrane, again exemplifying the strong interaction between the peptide pair.

#### Distinctive character of the peptide pair in a mixed population of cells

To test the selectivity of the K3-functionalized vesicles towards cells bearing the complementary peptide, a mixture of CPE-functionalized and unfunctionalized cells was incubated with K3-functionalized vesicles. In this experiment, a part of the cells in a 96 well plate was blocked with a Teflon tube and the area around it was functionalized with CPE. Cells were then

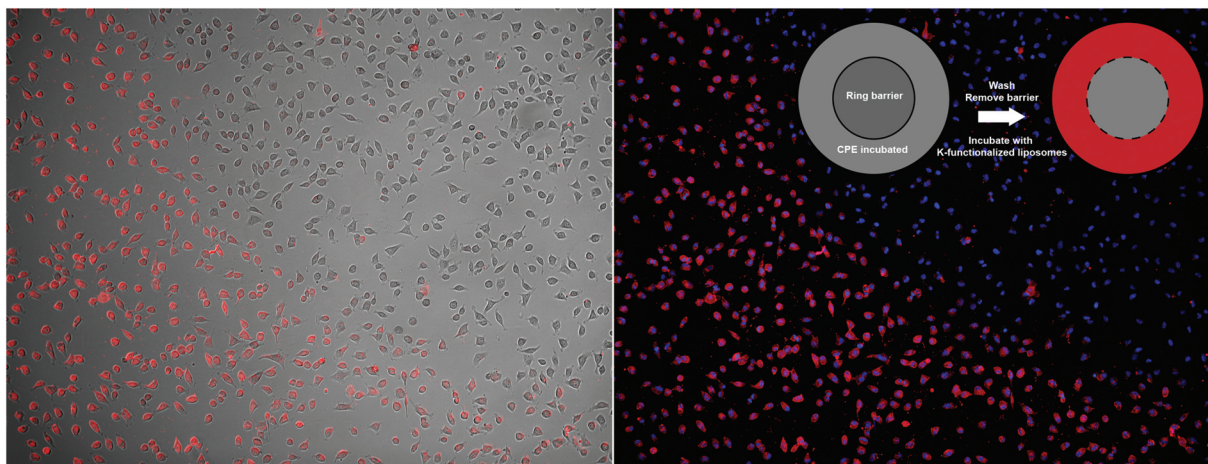


**Fig. 4** Adherent CPE-functionalized and unfunctionalized HeLa pLuc705 cells incubated with rhodamine-labeled K3-functionalized vesicles. After seeding, part of the well (96 well plate) was blocked using a Teflon ring. Outside this barrier, cells were incubated with CPE. After washing, the barrier was removed and the entire well was incubated with rhodamine-labeled K3-functionalized vesicles (inset). Overlays with the brightfield picture (left) and with the Hoechst nuclear staining (right) show that the CPE-functionalized cells were labeled red and the outer rim of the area where the barrier was positioned was clearly visible.

washed and after the barrier was removed, they were incubated with labeled K3-functionalized vesicles. When pictures were taken using a microscope there was a very clear difference in liposome binding between the CPE-functionalized cells and the unfunctionalized cells (Fig. 4). The round shape of the barrier could easily be recognized in the binding pattern indicating no diffusion or cross-over of the anchor and no off-target binding of the liposomes.

Because there may be more diffusion and cross-over in solution, a complementary experiment was performed with cells in suspension. HeLa pLuc705 cells were counted and then split, after which half of them were incubated with CPE and the other half with a control medium containing calcein-AM to distinguish between the two populations, also before incubation with the vesicles. After washing, the cells were pooled in a one to one ratio and incubated with K3-functionalized

vesicles. After another washing step, the cells were imaged under the microscope in suspension (Fig. 5).

Also in suspension, two different populations could be distinguished. The green labeled unfunctionalized cells did not show any interaction with the vesicles whereas the functionalized cells were clearly labeled red. The red labeled cells cluster more than the unfunctionalized cells, which could indicate that there is some homo-coiling of the CPE peptides in the functionalized cells, or that the K3-functionalized vesicles are crosslinking the cells, similar to as was seen in the aggregation assay with K3- and E3-functionalized vesicles (Fig. 2). When monitoring over a timeframe of 15 minutes, it was seen that membrane labeling starts immediately after addition of the labeled liposomes. A video of the increasing red fluorescence over time is available in the ESI (Videos S1 and S2<sup>†</sup>).

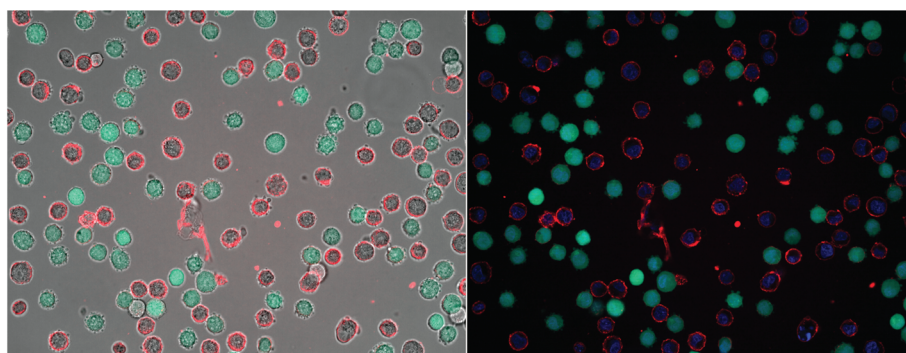


**Fig. 5** Mixed population of CPE-functionalized and unfunctionalized HeLa pLuc705 cells incubated with rhodamine-labeled K3-functionalized vesicles in suspension. Unfunctionalized cells were incubated with calcein-AM to distinguish between the two populations. Overlays with the brightfield picture (left) and with the Hoechst nuclear staining (right) show that the CPE-functionalized cells were clearly labeled red while the other population that was not functionalized had no detectable interaction with the vesicles at all.

The cells in these experiments had the exact same background and thus membrane proteins and receptors, with the CPE peptide as the only difference. The ability to distinguish between these two cell populations both in adherent cells and in suspension demonstrates the high specificity of the peptide pair. This allows for new possibilities to selectively target cells in the same vessel, regardless of any existing cell surface properties.

### Functional delivery of nucleic acid payloads after docking

When docking was successfully demonstrated, it was tested whether these vesicles and the coiled coil interaction could be used to functionally deliver model nucleic acid payloads. For delivery of the single stranded oligonucleotide (SCO), the HeLa pLuc705 cell line was used. This cell line is stably transfected with a luciferase gene that is interrupted by a mutated human  $\beta$ -globin intron 2 (IVS2-705), described by Kang *et al.*<sup>34</sup> Under normal conditions, this results in the encounter of a premature stop codon and the expression of a truncated, non-functional luciferase protein. When the 705 exon skipping SCO is successfully delivered, the splicing site (at position 705) is masked and the unnatural exon is spliced out, resulting in the restoration of luciferase expression.<sup>34</sup> For the delivery of conventional siRNA, a HeLa cell line stably expressing a luciferase construct was used.<sup>35</sup> Similar to the microscopy experiments, the cells were incubated with the CPE or CPK lipopeptide but then followed by incubation with SCO or siRNA loaded liposomes, functionalized with K3, E3 or unfunctionalized. After the transfection experiments, cells were lysed and luciferase expression was measured.

Successful transfection and restoration of luciferase expression were demonstrated when the HeLa pLuc705 cells were modified with CPE and the SCO loaded vesicles were functionalized with the K3-peptide. K3-functionalized vesicles

did not transfect the unfunctionalized cells. When compared to the positive control Lipofectamine 2000, the efficiency of exon-skipping is approximately 60%. Unfunctionalized vesicles did not deliver the nucleic acid cargo and neither did the E3-functionalized vesicles to the CPK modified cells (Fig. 6). This was also seen in the docking experiment and this again shows that the effect is dependent on coiled coil formation of the complementary peptides. The same peptide dependency is seen when siRNA is delivered to the HeLa PGK-Luciferase cells, however, the silencing effect when compared to lipofectamine was only 25% (Fig. 7).

What is of more importance is the mechanism by which these vesicles deliver the nucleic acids. Clearly, the docking of the peptides is important, since unfunctionalized vesicles do not transfect. A logical explanation would be that docking of vesicles at the cell membrane triggers a direct fusion mechanism with the cell membrane, thereby delivering the splice correcting oligonucleotide. The fusion of natural membranes is initiated by SNARE proteins that pull the opposing membranes in juxtaposition.<sup>6,7</sup> That could also be the mechanism of delivery for the vesicles in the present work, but herein, the peptides are on the distal end of a PEG polymer (MW  $\sim$  2000, PEG<sub>45</sub>) so the two membranes are in fact not that close. In the work of Pähler *et al.*, the effect of parallel *versus* anti-parallel docking of the E3/K3 pair on synthetic vesicles was investigated.<sup>42</sup> Half of the peptides were synthesized in the reverse order, such that when the peptides assembled, the N- and C-termini were together (anti-parallel docking) as opposed to the two N-termini in the normal situation (parallel docking). It was found that the anti-parallel coil assembly only resulted in docking while the parallel orientation also led to fusion (defined as the exchange of lipids and aqueous content between the different vesicle populations).<sup>42</sup> This was explained by the increased distance between the bilayers when

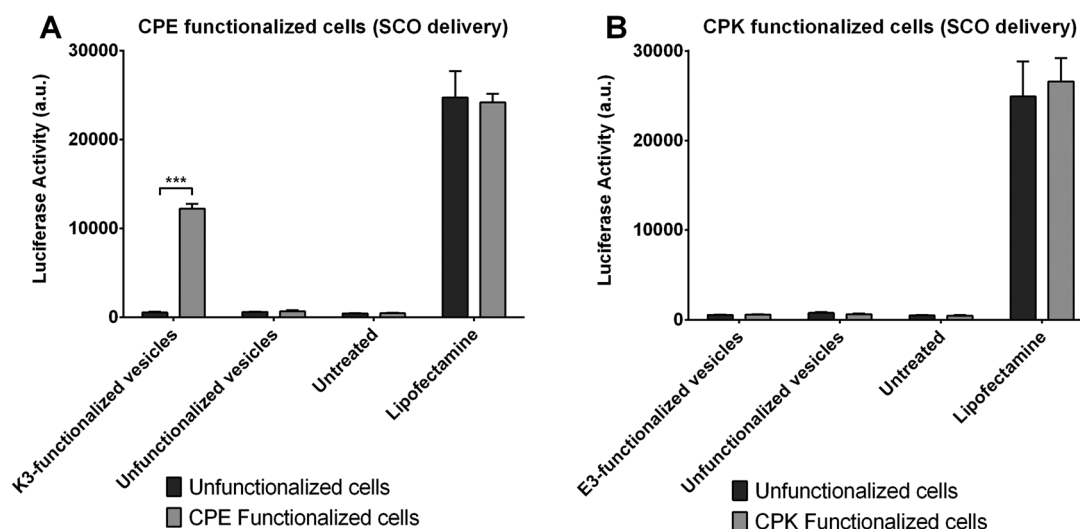
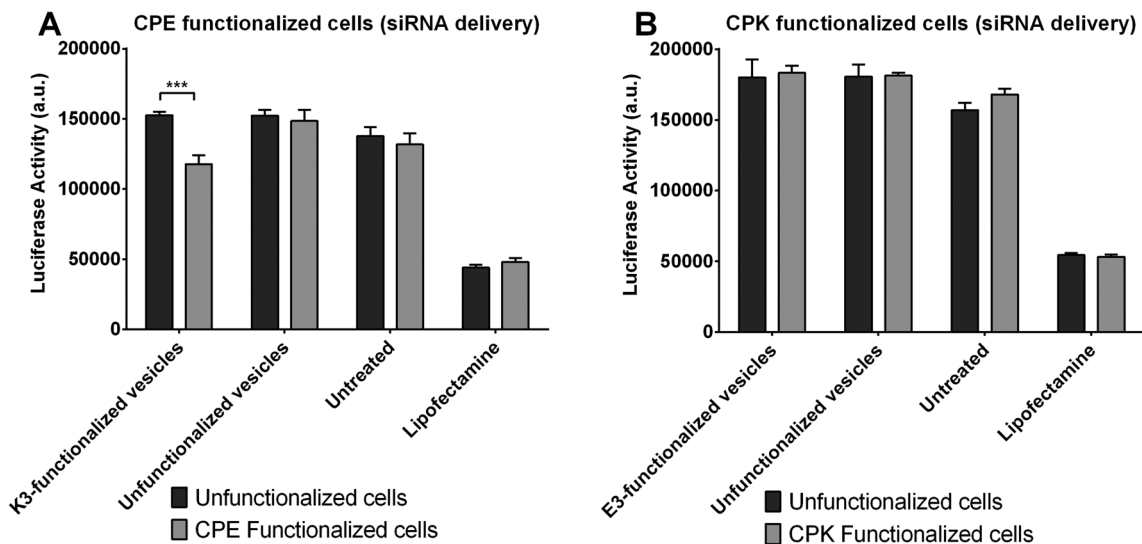


Fig. 6 Luciferase expression in HeLa pLuc705 cells after transfections with SCO loaded vesicles. Baseline expression was low and was restored after successful transfection. Grey bars represent CPE modified cells (left) and CPK modified cells (right). Black bars represent unfunctionalized cells (\*\*\*) denotes  $p < 0.001$ .





**Fig. 7** Luciferase silencing in HeLa PGK-Luciferase cells after transfections with siRNA loaded vesicles. Baseline expression is high and is silenced after successful transfection. Grey bars represent CPE modified cells (left) and CPK modified cells (right). Black bars represent unfunctionalized cells (\*\*\*) denotes  $p < 0.001$ ).

the peptides dock anti-parallel and in that work, the peptides were conjugated directly to the bilayer, without any additional PEG spacer like in our work. Therefore, with our PEGylated vesicles, it is not likely that the membranes are brought in direct contact immediately after docking.

To investigate the delivery mechanism, microscopy images of the labeled vesicles, docked to the cells were taken over time to monitor cellular uptake. When the cells are imaged directly after incubation, a very clear, homogeneously distributed membrane labeling is seen (Fig. 8).

After one hour, the membrane labeling is less clear and bright red spots appear, indicating that the vesicles are in fact taken up in endosomal compartments. After four hours of incubation, which corresponds with the incubation time in transfection studies, the membrane labeling becomes much less intense, while the endosomal spots become much more

prominent and numerous. These pictures show that despite the absence of a downstream signaling cascade, the vesicles are actively taken up, possibly by non-specific uptake mechanisms such as macropinocytosis or membrane recycling mechanisms.

## Discussion and conclusion

The results presented here show that the highly distinctive interaction between the K3- and E3-peptides and more specifically, the interaction between K3-functionalized vesicles and CPE-functionalized cells, can lead to the functional delivery of two types of small oligonucleotides that normally do not cross the cellular membrane. It was demonstrated that merely the docking to the cell membrane and the coiling of the peptide

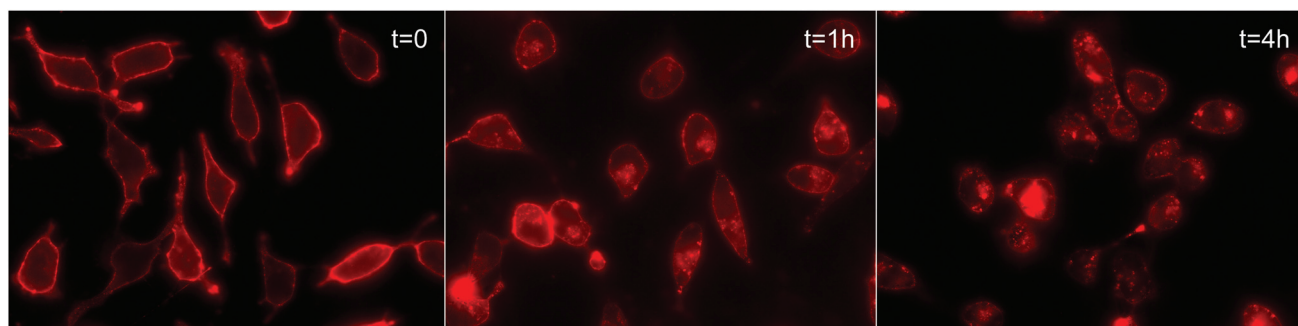


**Fig. 8** Microscopy pictures of CPE-functionalized HeLa pLuc705 cells incubated with K3-functionalized rhodamine-labeled vesicles over time. Directly after adding the vesicles, the cell membrane is clearly and homogeneously labeled. After one hour of incubation, brightly colored compartments start to appear. After four hours, the membrane labeling almost disappears and more numerous and brighter compartments are now visible, indicating an active uptake of the vesicles over time.

pair at the cell surface, leads to uptake in endocytic vesicles and eventually to cytosolic delivery. Furthermore, this interaction is specific enough to distinguish between cells of an identical background in the same vial that were or were not functionalized with the complementary peptide. This discrimination is independent of any existing surface protein expression and allows for highly specific cell binding and recognition.

Alternative to our approach of inserting the CPE lipopeptide into the cell membrane, the peptide could be recombinantly expressed to tag specific cell subsets and to obtain a highly targeted docking of liposomes to their cell membranes required as a first step towards the targeted delivery of nucleic acids.<sup>39</sup> For an *in vivo* application however, this would require another transfection with another targeted vector in order to get this artificial construct expressed on the target cell first. A more viable two-step approach was described by the group of Kopeček, where one of the coil forming peptides was fused to a Fab' fragment and in this way docked on the target cells *in vitro* and *in vivo*. A polymer functionalized with the complementary peptide could then interact with its target cell through an assembly of the peptides.<sup>18,19</sup> This approach was also shown to be feasible *in vivo* and could be combined with imaging applications.<sup>20,21</sup> Another *in vivo* application is inspired by the very interesting work by Raemdonck *et al.* in which "hitchhiking nanoparticles" are described.<sup>43</sup> In that work, lipid nanoparticles were reversibly coupled to isolated cytotoxic T-lymphocytes that are known to migrate to the tumor upon re-administration to the body. In this way, the concentration of nanoparticles in the tumor is increased. The cholesterol lipopeptide could be an alternative way to functionalize the lymphocytes *ex vivo* and the very high affinity and specificity of the peptide pair that was demonstrated in the present work, could aid the nanoparticles in hitchhiking to the tumor area.

Expanding on this, there are many other applications where cells are manipulated *ex vivo* that could benefit from a highly specific non-viral gene delivery system to modify the cells of interest. For example, T-cells can be re-directed by transferring T-cell receptor genes, or by transducing them with chimeric antigen receptors.<sup>44</sup> Another important example is the gene editing system CRISPR/Cas9 which at this point also appears to have more *ex vivo* applications than *in vivo* use due to the current high off-target mutagenesis.<sup>45</sup> So far it has been used to inactivate latent HIV-infections in primary T-cells<sup>46</sup> and to correct the dystrophin gene in Duchenne's Muscular Dystrophy patient-derived induced pluripotent stem cells.<sup>47,48</sup>

To summarize, there is a growing interest in the *ex vivo* manipulation of cells, both on the cell surface as well as at the genomic level, to use them as a targeted delivery system. These applications can benefit from a highly selective, non-viral delivery system that is capable of functionally delivering nucleic acid cargos. This work shows the proof of concept that such molecules can be delivered using an artificial coiled coil forming targeting system that is independent of any existing cell surface properties or genetic background.

## Acknowledgements

The research leading to these results has received support from the Innovative Medicines Initiative Joint Undertaking under grant agreement no. 115363 (IMI-COMPACT), resources of which are composed of financial contribution from the European Union's Seventh Framework Programme (FP7/2007-2013) and EFPIA companies in kind contribution. A. K. acknowledges the financial support of the Netherlands Organization of Scientific Research (NWO) *via* a VICI grant.

## References

- 1 A. L. Boyle and D. N. Woolfson, *Chem. Soc. Rev.*, 2011, **40**, 4295–4306.
- 2 B. Apostolovic, M. Danial and H.-A. Klok, *Chem. Soc. Rev.*, 2010, **39**, 3541–3575.
- 3 S. Cavalli, F. Albericio and A. Kros, *Chem. Soc. Rev.*, 2010, **39**, 241–263.
- 4 H. Robson Marsden and A. Kros, *Angew. Chem., Int. Ed.*, 2010, **49**, 2988–3005.
- 5 J. M. Mason and K. M. Arndt, *ChemBioChem*, 2004, **5**, 170–176.
- 6 R. Jahn and R. H. Scheller, *Nat. Rev. Mol. Cell Biol.*, 2006, **7**, 631–643.
- 7 F. Li, F. Pincet, E. Perez, W. S. Eng, T. J. Melia, J. E. Rothman and D. Tareste, *Nat. Struct. Mol. Biol.*, 2007, **14**, 890–896.
- 8 C. Fortier, G. De Crescenzo and Y. Durocher, *Biomaterials*, 2013, **34**, 1344–1353.
- 9 E. Zacco, J. Hütter, J. L. Heier, J. Mortier, P. H. Seeberger, B. Lepenies and B. Koksich, *ACS Chem. Biol.*, 2015, **10**, 2065–2072.
- 10 Y. Assal, Y. Mizuguchi, M. Mie and E. Kobatake, *Bioconjugate Chem.*, 2015, **26**, 1672–1677.
- 11 J. M. Fletcher, R. L. Harniman, F. R. H. Barnes, A. L. Boyle, A. Collins, J. Mantell, T. H. Sharp, M. Antognozzi, P. J. Booth, N. Linden, M. J. Miles, R. B. Sessions, P. Verkade and D. N. Woolfson, *Science*, 2013, **340**, 595–599.
- 12 H. Gradišar, S. Božič, T. Doles, D. Vengust, I. Hafner-Bratkovič, A. Mertelj, B. Webb, A. Šali, S. Klavžar and R. Jerala, *Nat. Chem. Biol.*, 2013, **9**, 362–366.
- 13 M. Pechar, R. Pola, R. Laga, A. Braunová, S. K. Filippov, A. Bogomolova, L. Bednárová, O. Vaněk and K. Ulbrich, *Biomacromolecules*, 2014, **15**, 2590–2599.
- 14 U. I. M. Gerling-Driessen, N. Mujkic-Ninnemann, D. Ponader, D. Schöne, L. Hartmann and B. Koksich, *Biomacromolecules*, 2015, **16**, 2394–2402.
- 15 E. Zacco, C. Anish, C. E. Martin, H. V. Berlepsch, E. Brandenburg, P. H. Seeberger and B. Koksich, *Biomacromolecules*, 2015, **16**, 2188–2197.
- 16 T. A. P. F. Doll, T. Neef, N. Duong, D. E. Lanar, P. Ringler, S. A. Müller and P. Burkhard, *Nanomed. Nanotechnol. Biol. Med.*, 2015, 1–10.
- 17 W. Shen, K. Zhang, J. A. Kornfield and D. A. Tirrell, *Nat. Mater.*, 2006, **5**, 153–158.

- 18 K. Wu, J. Liu, R. N. Johnson, J. Yang and J. Kopeček, *Angew. Chem., Int. Ed.*, 2010, **49**, 1451–1455.
- 19 T.-W. Chu, J. Yang and J. Kopeček, *Biomaterials*, 2012, **33**, 7174–7181.
- 20 K. Wu, J. Yang, J. Liu and J. Kopeček, *J. Controlled Release*, 2012, **157**, 126–131.
- 21 R. Zhang, J. Yang, T.-W. Chu, J. M. Hartley and J. Kopeček, *Adv. Healthcare Mater.*, 2015, **4**, 1054–1065.
- 22 B. Tripet, L. Yu, D. L. Bautista, W. Y. Wong, R. T. Irvin and R. S. Hodges, *Protein Eng.*, 1996, **9**, 1029–1042.
- 23 H. Chao, D. L. Bautista, J. Litowski, R. T. Irvin and R. S. Hodges, *J. Chromatogr., B: Biomed. Appl.*, 1998, **715**, 307–329.
- 24 H. Robson Marsden, N. A. Elbers, P. H. H. Bomans, N. A. J. M. Sommerdijk and A. Kros, *Angew. Chem., Int. Ed.*, 2009, **48**, 2330–2333.
- 25 F. Versluis, J. Voskuhl, B. Van Kolck, H. Zope, M. Bremmer, T. Albrechtse and A. Kros, *J. Am. Chem. Soc.*, 2013, **135**, 8057–8062.
- 26 H. Robson Marsden, A. V. Korobko, T. Zheng, J. Voskuhl and A. Kros, *Biomater. Sci.*, 2013, **1**, 1046.
- 27 H. R. Zope, F. Versluis, A. Ordas, J. Voskuhl, H. P. Spaink and A. Kros, *Angew. Chem., Int. Ed.*, 2013, **52**, 14247–14251.
- 28 L. Kong, S. H. C. Askes, S. Bonnet, A. Kros and F. Campbell, *Angew. Chem., Int. Ed.*, 2016, **55**, 1396–1400.
- 29 N. Lopez Mora, A. Bahreman, H. Valkenier, H. Li, T. Sharp, D. N. Sheppard, A. Kros and A. Davis, *Chem. Sci.*, 2016, **7**, 1768–1772.
- 30 N. Maurer, K. F. Wong, H. Stark, L. Louie, D. McIntosh, T. Wong, P. Scherrer, S. C. Semple and P. R. Cullis, *Biophys. J.*, 2001, **80**, 2310–2326.
- 31 J. N. Moreira, T. Ishida, R. Gaspar and T. M. Allen, *Pharm. Res.*, 2002, **19**, 265–269.
- 32 E. G. Bligh and W. Dyer, *Can. J. Biochem. Physiol.*, 1959, **37**, 911–917.
- 33 G. Rouser, S. Fleischer and A. Yamamoto, *Lipids*, 1970, **5**, 494–496.
- 34 S. H. Kang, M. J. Cho and R. Kole, *Biochemistry*, 1998, **37**, 6235–6239.
- 35 B. Su, A. Cengizeroglu, K. Farkasova, J. R. Viola, M. Anton, J. W. Ellwart, R. Haase, E. Wagner and M. Ogris, *Mol. Ther.*, 2013, **21**, 300–308.
- 36 I. M. Hafez, N. Maurer and P. R. Cullis, *Gene Ther.*, 2001, **8**, 1188–1196.
- 37 K. W. C. Mok, A. M. I. Lam and P. R. Cullis, *Biochim. Biophys. Acta, Biomembr.*, 1999, **1419**, 137–150.
- 38 E. A. Smith and J. C. Weisshaar, *Biophys. J.*, 2011, **100**, 2141–2150.
- 39 Y. Yano, A. Yano, S. Oishi, Y. Sugimoto, G. Tsujimoto, N. Fujii and K. Matsuzaki, *ACS Chem. Biol.*, 2008, **3**, 341–345.
- 40 M. Rabe, C. Schwieger, H. R. Zope, F. Versluis and A. Kros, *Langmuir*, 2014, **30**, 7724–7735.
- 41 M. Rabe, H. R. Zope and A. Kros, *Langmuir*, 2015, **31**, 9953–9964.
- 42 G. Pähler, C. Panse, U. Diederichsen and A. Janshoff, *Biophys. J.*, 2012, **103**, 2295–2303.
- 43 L. Wayteck, H. Dewitte, L. De Backer, K. Breckpot, J. Demeester, S. C. De Smedt and K. Raemdonck, *Biomaterials*, 2016, **77**, 243–254.
- 44 W. J. Urba and D. L. Longo, *N. Engl. J. Med.*, 2011, **365**, 754–757.
- 45 N. Savić and G. Schwank, *Transl. Res.*, 2016, **168**, 15–21.
- 46 H.-K. Liao, Y. Gu, A. Diaz, J. Marlett, Y. Takahashi, M. Li, K. Suzuki, R. Xu, T. Hishida, C.-J. Chang, C. R. Esteban, J. Young and J. C. Izpisua Belmonte, *Nat. Commun.*, 2015, **6**, 6413.
- 47 D. G. Ousterout, A. M. Kabadi, P. I. Thakore, W. H. Majoros, T. E. Reddy and C. A. Gersbach, *Nat. Commun.*, 2015, **6**, 6244.
- 48 H. L. Li, N. Fujimoto, N. Sasakawa, S. Shirai, T. Ohkame, T. Sakuma, M. Tanaka, N. Amano, A. Watanabe, H. Sakurai, T. Yamamoto, S. Yamanaka and A. Hotta, *Stem Cell Rep.*, 2015, **4**, 143–154.